# Mixer Imbalance Correction in Wireless OFDM Systems

Chris Hall
*Department of Electrical and Computer Engineering*
*University of Arizona*
Tucson, United States
Chris93Hall@email.arizona.edu

Ivan Djordjevic
*Department of Electrical and Computer Engineering*
*University of Arizona*
Tucson, United States
Ivan@arizona.edu

***Abstract*—In this paper we present an improved method for correcting mixer imbalance in wireless systems using Orthogonal Frequency Division Multiplexing (OFDM). Mixer imbalance causes a nonlinear distortion to complex baseband signals. We start by introducing several mathematical models for mixer imbalance in the time domain. Then we select the most appropriate one of the time domain models and use it to develop a frequency domain model. We show that when observed in the frequency domain, mixer imbalance causes intersubcarrier interference as well as interference between the in phase and quadrature components of each individual subcarrier. Our improved method of correcting for these effects takes advantage of symmetries in the interference parameters. These symmetries allow for better estimation of the interference which in turn allows for better recovery of the transmitted symbols. We show that for a given set of mixer imbalance parameters there is a minimum SNR at which imbalance correction will improve symbol recovery. The exact value for the threshold SNR depends on the imbalance parameter estimation method used. The method proposed here lowers that threshold SNR at which improved symbol recovery begins compared to a previously proposed method. Error Vector Magnitude (EVM) and Symbol Error Rate (SER) are the metrics we used to evaluate our proposed method.**

***Index Terms*—OFDM, mixer imbalance, wideband, millimeter wave, advanced PHY techniques**

## I. Introduction

WIDEBAND communication systems at high carrier frequencies are particularly susceptible to mixer imbalance, which can significantly impair the channel and negatively impact capacity. Ultrawideband communications systems are gaining popularity in research and industry due to the establishment of massive licensed and unlicensed bands at higher frequencies by the FCC.

DACs and ADCs with sample rates high enough to support a desired ultrawideband system at the correct cost point can be a challenge. One tradeoff that sometimes makes sense is to use a direct to baseband architecture instead of an intermediate frequency architecture typically used in modern communications devices. The tradeoff is to cut the ADC and DAC bandwidth requirements in half at the expense of requiring two of each and a superheterodyne mixer. In direct to baseband architectures, mixer imbalance can be a major source of signal distortion. Mixer imbalance on the receive and transmit ends of a communication system distort the received signal, and result in more symbol erors than would be caussed by Gaussian noise alone.

There are a number of published works in this area. Some work focuses on correction of mixer imbalance present at either the transmitter or the receiver, but not both [1,2]. Another common simplifying constraint is to assume a narrowband system. Other research relys on a complex hardware feedback loop on the receiver or transmitter in order to measure the imbalance parameters directly.

The imbalance problem can be avoided by mixing down to an intermediate frequency and directly sampling the IF signal. The tradeoff here is that it requires a single ADC at twice the bandwidth as opposed to two ADCs at half the bandwidth with direct down conversion. Implementing a two stage down conversion architecture is another technique to partially mitigate the effects of mixer imbalance and reduce the ADC/DAC bandwidth requirements at the cost of added hardware complexity [3]. The direct down conversion and direct up conversion architectures that we are concerned about in this paper suffer most from the mixer imbalance problem but also strikes a nice middle ground of hardware complexity while keeping ADC/DAC bandwidth requirements low [4].

There are a couple easily recognizable indicators that a communication system may be mixer imbalance limited as opposed to thermal noise limited. If shortening the transmit distance does not improve the constellation diagram, the system might be mixer imbalance limited. If increasing transmit power does not improve the constellation diagram, it might be mixer imbalance limited. If swapping in higher quality hardware components in an attempt to increase SNR does not result in a better looking constellation, it might be mixer imbalance limited. As we will show later, a less obvious indicator is that specific OFDM subcarriers will have a nonzero cross correlation.

In this paper we tackle the problem of correcting for both transmit and receive mixer imbalance present in a wideband communication system using OFDM signaling. Our solution is a modification to a previously proposed solution to the same problem [5].

We will start by defining two equivalent mathematical models to describe mixer imbalance. Then we will choose one and use it to describe the frequency domain effects on

a transmitted signal. Next we propose an improved method for correcting for the frequency domain effects for the case where OFDM symbols are transmitted, and estimating the sent symbols. We make some claims about the structure of the equalization matrix. Finally, we choose a set of parameters and present some illustrative simulation results which show the performance improvements of our method compared to other techniques.

## II. Mathematical Models

There are two different, but equivalent, models to describe mixer imbalance in the time domain. The first model assumes that the transmiter and receiver mixers have perfect passthrough of the in-phase component of the signal without any amplitude or phase imbalance. All of the imbalance is contributed to the quadrature component of the signal. The second model splits the imbalance between the in-phase and the quadrature components.

For reference, the ideal upmixing model is given by

$$s(t) = Re\{x\}\cos(2\pi f_c t) + Im\{x\}\sin(2\pi f_c t), \quad (1)$$

while the ideal downmixing model is

$$y(t) = LPF\{s(t)\cos(2\pi f_c t) + is(t)\sin(2\pi f_c t)\}. \quad (2)$$

Here LPF is a lowpass filter opperation. In the absence of noise and mixer imbalance, the received signal $y(t)$ should match $x(t)$ to a scale factor. In the rest of this paper we will use a matrix notation to show the transformation of the transmit signal, $x(t)$, to the received signal, $y(t)$. This matrix notation will break apart the real and imaginary components to show how each one is affected differently. For this ideal case, the matrix model would look as follows.

$$\begin{bmatrix} y_I \\ y_Q \end{bmatrix} = \begin{bmatrix} 1 & 0 \\ 0 & 1 \end{bmatrix} \begin{bmatrix} x_I \\ x_Q \end{bmatrix} \quad (3)$$

Here the channel matrix, $H$, is the identity matrix. This is the baseband equivalent model for a communication system with no mixer impairments and no channel effects. For much of the rest of this paper we will drop the dependent and independent variables on the left and right hand side of the transform matrix and focus only on $H$ itself.

### A. First Form

The first mixer imbalance model we will define is the same model used in previous work [5]. We define the in-phase components of both the receiver and transmitter to exist without impairments. Then all the impairments must exist in the quadrature components, as given by Eqs. (4) and (5). This model is valid because the significant concept in mixer imbalance is the relative difference in magnitude and phase impairments between the in-phase and quadrature components.

$$s(t) = Re\{x\}\cos(2\pi f_c t) + Im\{x\}(1+\alpha_T)\sin(2\pi f_c t + \phi_T) \quad (4)$$

$$y(t) = LPF\{s(t)\cos(2\pi f_c t) + is(t)(1+\alpha_R)\sin(2\pi f_c t + \phi_R)\} \quad (5)$$

The constants $\alpha_T$ and $\alpha_R$ are the amplitude imbalance in the transmit and receive mixers respectively. The phase constants $\phi_T$ and $\phi_R$ describe the phase imbalances in the transmit and receive mixers respectively.

We can work the math into a matrix form, given by Eq. (6), similar to that shown above for an ideal channel and then decompose that two by two matrix into four component matricies. Each of the component matricies represent receive amplitude, receive phase, transmit phase, and transmit amplitude imbalance respectively.

$$\begin{bmatrix} 1 & 0 \\ 0 & \alpha_R \end{bmatrix} \begin{bmatrix} 1 & 0 \\ \sin(\phi_R) & \cos(\phi_R) \end{bmatrix} \begin{bmatrix} 1 & \sin(\phi_T) \\ 0 & \cos(\phi_T) \end{bmatrix} \begin{bmatrix} 1 & 0 \\ 0 & \alpha_T \end{bmatrix} \quad (6)$$

### B. Second Form

The second form assumes symetrical errors in the in phase and quadrature components, so that we can write:

$$\begin{aligned} s(t) = Re\{x\}(1+\frac{\alpha_T}{2})\cos(2\pi f_c t - \frac{\phi_T}{2}) + \\ Im\{x\}(1-\frac{\alpha_T}{2})\sin(2\pi f_c t - \frac{\phi_T}{2}) \end{aligned} \quad (7)$$

$$\begin{aligned} y(t) = LPF\{s(t)(1+\frac{\alpha_R}{2})\cos(2\pi f_c t + \\ \frac{\phi_R}{2}) + is(t)(1-\frac{\alpha_R}{2})\sin(2\pi f_c t - \frac{\phi_R}{2})\} \end{aligned} \quad (8)$$

By re-arranging the equations a little, we can get a matrix form for this transformation:

$$H = \begin{bmatrix} H_{II} & H_{IQ} \\ H_{QI} & H_{QQ} \end{bmatrix} \quad (9)$$

$$H_{II} = (1+\alpha_T)(1+\alpha_R)\cos(\phi_T - \phi_R) \quad (10)$$

$$H_{IQ} = (1-\alpha_T)(1+\alpha_R)\sin(-\phi_T - \phi_R) \quad (11)$$

$$H_{QI} = (1+\alpha_T)(1-\alpha_R)\sin(-\phi_T - \phi_R) \quad (12)$$

$$H_{QQ} = (1-\alpha_T)(1-\alpha_R)\cos(-\phi_T + \phi_R) \quad (13)$$

Similarly to the first model, this matrix can be factored into 4 separate matricies, representing the effects of phase imbalance and amplitude imbalance at both the recieve end and the transmit end:

$$\begin{bmatrix} 1+\alpha_R & 0 \\ 0 & 1-\alpha_R \end{bmatrix} \begin{bmatrix} \cos(-\phi_R) & \sin(-\phi_R) \\ \sin(-\phi_R) & \cos(-\phi_R) \end{bmatrix} \begin{bmatrix} \cos(-\phi_T) & \sin(-\phi_T) \\ \sin(-\phi_T) & \cos(-\phi_T) \end{bmatrix} \begin{bmatrix} 1+\alpha_T & 0 \\ 0 & 1-\alpha_T \end{bmatrix} \quad (14)$$

$$H_{Total} = A_{RX} Q_{RX} Q_{TX} A_{TX} \tag{15}$$

We can add channel effects to this model by inserting an extra matrix in the middle. For this model we will assume the channel is linear, time invariant, and memoryless. The memoryless property is realistic for narrowband channels so we can write

$$H_{Total} = A_{RX} Q_{RX} H Q_{TX} A_{TX} \tag{16}$$

Here $H$ takes the form of a rotation matrix with a gain:

$$h = |h| e^{i\angle h} \Rightarrow H = \begin{bmatrix} |h|\cos(\angle h) & |h|\sin(\angle h) \\ -|h|\sin(\angle h) & |h|\cos(\angle h) \end{bmatrix} \tag{17}$$

This time domain model assumes the channel can be accuretly represented by a frequency flat model. In other words, the channel must be memoryless and time invariant. These conditions are generally assumed for narrowband communications, but do not hold true for wideband opperations.

Due to the interference between the in-phase and quadrature components, $H_{Total}$ is not a rotation matrix. However, any 2x2 matrix can be decomposed into the sum of a complex linear component (rotation marix) and a complex nonlinear component with the intent of minimizing the magnitude of the nonlinear component:

$$\begin{bmatrix} a & b \\ c & d \end{bmatrix} = \begin{bmatrix} e & -f \\ f & e \end{bmatrix} + \begin{bmatrix} g & h \\ i & j \end{bmatrix} \tag{18}$$

The conventional zero forcing method for estimating a complex channel would look like this:

$$\frac{y_I + iy_Q}{x_I + ix_Q} = |h| e^{i\angle h} \rightarrow \begin{bmatrix} |h|\cos(\angle h) & |h|\sin(\angle h) \\ -|h|\sin(\angle h) & |h|\cos(\angle h) \end{bmatrix} \neq \begin{bmatrix} e & -f \\ f & e \end{bmatrix} \tag{19}$$

The zero forcing method will always yield a rotation matrix.

Not only does the zero forcing estimate not equal to the linear component of the decomposed nonlinear model, but it actually depends on your choice of $x$ used to excite the model with.

## III. Frequency Domain Effects

If we want to observe the frequency domain effects of mixer imbalance, we can define a DFT matrix $D_n$ of length $n$ such that $D_n D_n^{-1} = I_n$ so that we can write:

$$H_{Total} = D_n A_{RX} Q_{RX} H Q_{TX} A_{TX} D_n^{-1} \tag{20}$$

Note that now $A_{RX}$, $A_{TX}$, $Q_{RX}$, $Q_{TX}$, and $H$ are block diagonal square matricies of size $n$. Furthermore, we can now model more complicated wideband channels by making $H$ a block Toeplitz matrix or by keeping it block diagonal and using the DFT matricies to create a frequency domain model as shown in Eq. (21). This change also allows us to represent

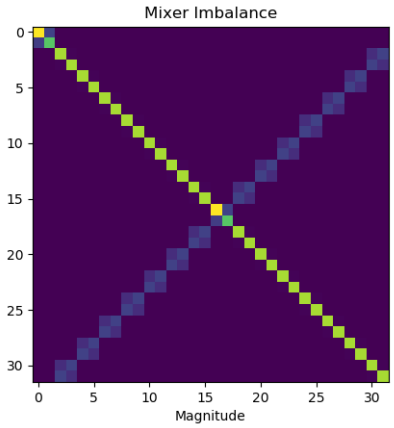


Fig. 1. Frequency domain effects with no channel

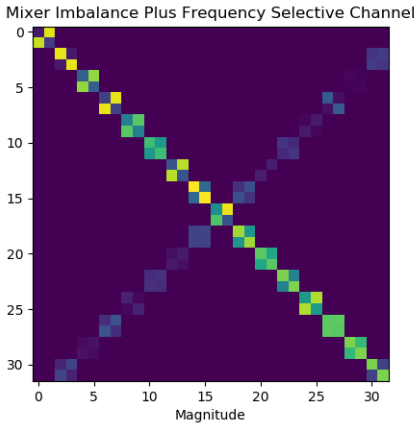


Fig. 2. Frequency domain effects with frequency selective channel

channels which are not frequency flat or memoryless. Keep in mind that every matrix in the equation above, including the DFT matricies, are in the real decomposed form described earlier.

$$H_{Total} = D_n A_{RX} Q_{RX} D_n^{-1} H D_n Q_{TX} A_{TX} D_n^{-1} \tag{21}$$

If we use this frequency domain representation to build a model that contains only mixer imbalance and no wireless channel effects, by setting $H$ equal to the identity matrix, we get a sparse matrix as shown in Fig. 1. Note how every subcarrier gets interference from at most one other subcarrier. In this case, since there are no wireless channel affects, every subcarrier sees the same interference structure.

When a frequency selective channel is chosen, and still using frequency invariant imbalance values, every subcarrier sees a different interference structure. However, the property of each subcarrier only getting interference from at most one other subcarrier still holds true, as shown in Fig. 2.

## IV. Proposed Method

The method we propose decomposes each of the complex subcarriers into two real values. Then we pair up the subcarriers according to the intercarrier interference shown in Figs. 1 and 2, see Eqs. (22),(23). Now, for each subcarrier pair, we have a linear system with four inputs, four outputs, and $H$ representing the channel effects between them as given by Eqn. (23).

$$y = Hx \tag{22}$$

So far, we have described the method proposed in previous works [5]. Our novel contribution is that the four by four $H$ matrix necessarily has a structure of repeating values. Knowledge of this structure aids us in more precisely estimating the transmitted symbols from a noisy reception.

$$H = \begin{bmatrix} c & d & g & -h \\ -d & c & -h & -g \\ a & -b & e & f \\ -b & -a & -f & e \end{bmatrix} \tag{23a}$$

$$x = \begin{bmatrix} x_{I0} \\ x_{Q0} \\ x_{I1} \\ x_{Q1} \end{bmatrix} \tag{23b}$$

In OFDM signaling, every subcarrier, other than the 0 and $\pi$ frequency subcarriers, gets interference from its reciprocal carrier and between its own real and imaginary components. The $H$ matrix defines the structure of the interference between the two reciprocal subcarriers.

Previous work did not investigate the structure of the $H$ matrix but instead attempted to predict each of the 16 elements of $H$ independently. Taking into account that each value in $H$ occurs twice, we can get a better estimate of these values in the presence of noise.

The approach we have taken here is to estimate the values of $H$ independently, via transmission of four OFDM training sequences, then take the average of each of the values that are supposed to be identical. The result of this averaging step is what we end up using in our $H$ matrix when equalizing new OFDM symbols.

We can calculate the unbiased estimator, $G$, as the Moore Penrose inverse of $H$ [6]:

$$G = \left(HH^T\right)^{-1} H \tag{24}$$

$G$ will have the same structure as we defined for $H$ above.

Once we have the estimator, $G$, we can convert it back into a complex estimator. First we split the estimator into one for the lower subcarrier and one for the upper subcarrier to get:

$$\begin{aligned} &\begin{bmatrix} c & d & g & -h \\ -d & c & -h & -g \end{bmatrix} \begin{bmatrix} y_{I0} \\ y_{Q0} \\ y_{I1} \\ y_{Q1} \end{bmatrix} \\ &= \begin{bmatrix} c & d & -h & g \\ -d & c & -g & -h \end{bmatrix} \begin{bmatrix} y_{I0} \\ y_{Q0} \\ y_{Q1} \\ y_{I1} \end{bmatrix} \end{aligned} \tag{25}$$

$$\begin{aligned} &\begin{bmatrix} a & -b & e & f \\ -b & -a & -f & e \end{bmatrix} \begin{bmatrix} y_{I0} \\ y_{Q0} \\ y_{I1} \\ y_{Q1} \end{bmatrix} \\ &= \begin{bmatrix} -b & a & e & f \\ -a & -b & -f & e \end{bmatrix} \begin{bmatrix} y_{Q0} \\ y_{I0} \\ y_{I1} \\ y_{Q1} \end{bmatrix} \end{aligned} \tag{26}$$

Recall that anything of the form

$$\begin{bmatrix} a & -b \\ b & a \end{bmatrix} \tag{27}$$

is reducable to a complex number, $|\alpha|e^{i\angle\alpha}$ where $\alpha$ is a complex exponential with $\angle\alpha = \tan^{-1}(a/b)$ and $|\alpha| = \frac{a}{\cos(\angle\alpha)}$, giving us the following two estimators:

$$\begin{bmatrix} \hat{x_{I0}} + \hat{x_{Q0}} \end{bmatrix} = \begin{bmatrix} |a|e^{i\angle a} & |b|e^{i\angle b} \end{bmatrix} \begin{bmatrix} y_{I0} + iy_{Q0} \\ y_{Q1} + iy_{I1} \end{bmatrix} \tag{28}$$

$$\begin{bmatrix} \hat{x_{I1}} + \hat{x_{Q1}} \end{bmatrix} = \begin{bmatrix} |c|e^{i\angle c} & |d|e^{i\angle d} \end{bmatrix} \begin{bmatrix} y_{Q0} + iy_{I0} \\ y_{I1} + iy_{Q1} \end{bmatrix} \tag{29}$$

Puting the estimator in this form does not gain us anything in terms of computational efficiency over the decomposed form we had before. But it helps to give us a more sound understanding and intuition of what is happening.

## V. Matrix Inverse Structure

For a square full rank matrix, the Moore Penrose inverse is also the inverse of the matrix [7].

If we have a four by four matrix, $H$, of the following form

$$\begin{bmatrix} a & b & c & -d \\ -b & a & -d & -c \\ e & -f & g & h \\ -f & -e & -h & g \end{bmatrix} \tag{30}$$

Then the inverse matrix, $H^{-1}$ will have a similar form:

$$H^{-1} = \frac{1}{det(H)} Adj(H) \tag{31}$$

The remainder of this calculation is simple but tedious and verbose, so it is left to the reader. The reader should arrive at the following result for $H^{-1}$:

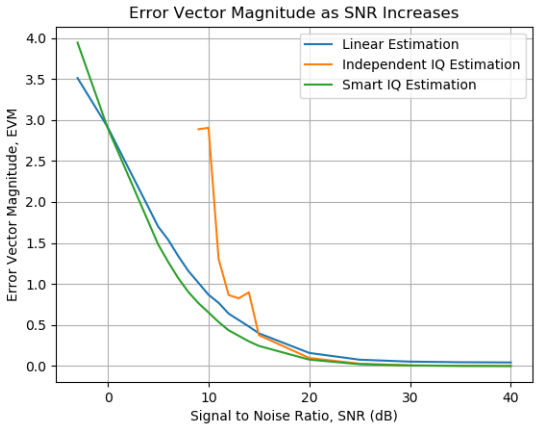


Fig. 3. Performance comparison against other methods

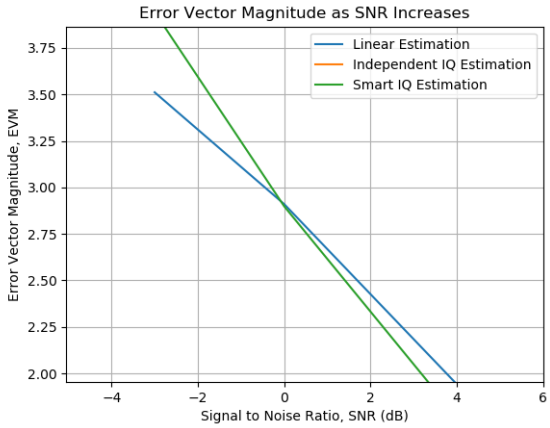


Fig. 4. Performance comparison against other methods (zoom lower SNR)

$$H^{-1} = \begin{bmatrix} H_{00}^{-1} & H_{01}^{-1} & H_{02}^{-1} & H_{03}^{-1} \\ H_{10}^{-1} & H_{11}^{-1} & H_{12}^{-1} & H_{13}^{-1} \\ H_{20}^{-1} & H_{21}^{-1} & H_{22}^{-1} & H_{23}^{-1} \\ H_{30}^{-1} & H_{31}^{-1} & H_{32}^{-1} & H_{33}^{-1} \end{bmatrix} = \begin{bmatrix} H_{00}^{-1} & H_{01}^{-1} & H_{02}^{-1} & H_{03}^{-1} \\ -H_{01}^{-1} & H_{00}^{-1} & H_{03}^{-1} & -H_{02}^{-1} \\ H_{20}^{-1} & H_{21}^{-1} & H_{22}^{-1} & H_{23}^{-1} \\ -H_{21}^{-1} & H_{20}^{-1} & H_{23}^{-1} & -H_{22}^{-1} \end{bmatrix} \tag{32}$$

This same structure also holds true for the larger block diagonal matrix we started with.

## VI. Illustrative Numerical Results

The following results are for an OFDM modulated system with 256 subcarriers per OFDM symbol. Each subcarrier has a symbol drawn from a QPSK constellation modulated onto it. Each subcarrier bandwidth is narrower than the coherence bandwidth of the channel. The cyclic prefix and guard intervals are long enough to handle the multipath delays. Our simulated system is modeled with frequency flat imbalance parameters $\alpha_T = 0.1$, $\alpha_R = 0.03$, $\phi_T = 0.05$, $\phi_R = 0.07$.

Fig. 3 is showing Error Vector Magnitude (EVM) as we sweep through SNR. Figs. 4 and 5 zoom in on important parts from Fig. 3 in order to highlight significant characteristics.

Right around 0 dB is where our method starts to outperform the linear zero forcing method of equalizing the channel. Our method always outperforms the previously suggested method of treating the I and Q channes independently, although at higher SNR they converge toward zero error. Additionally, the independent IQ estimation method becomes unstable at $SNR < 0$ dB in our example right around the point it becomes worse than traditional linear estimation.

It is important to note that no matter how high the SNR gets, the traditional linear zero forcing equalizer will never converge to zero Error Vector Magnitude. It will instead converge to some nonzero value dependent on the amount of mixer imbalance present. By contrast, at high SNR, independent IQ estimation approaches zero error as does the smart IQ estimation method proposed here.

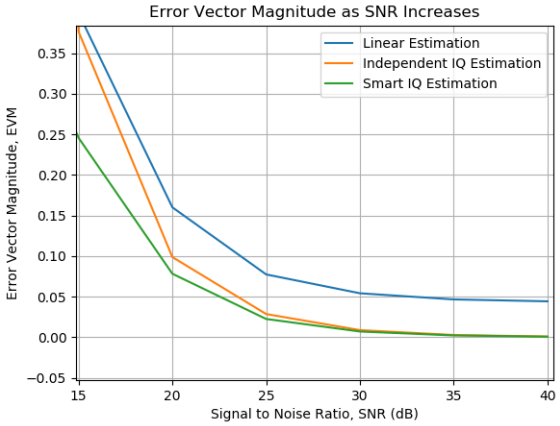


Fig. 5. Performance comparison against other methods (zoom higher SNR)

In Figs. 6 and 7 we have chosen an SNR value of 23 dB and plotted the constellation diagrams after equalization using each of the three methods. The first plot shows the traditional method of linear zero forcing. Notice that the range for this plot is larger than the other in order to include IQ samples farther from the origin. If we were to plot the constellation diagram for the method described in our previous work, we would see a tighter constellation than that given by the linear zero forcing method, but it would still shows a number of IQ samples that are close to the decision boundaries. The second constellation plot shows our proposed method, and has a healthier gap around the decision boundaries and tighter clustering.

We can generate a similar plot for Symbol Error Rate, however we need to crank up the imbalance values so that we can induce a meaningful number of errors in a QPSK constellation. The result in Fig. 8 is for a QPSK constellation and mixer imbalance parameters $\alpha_T = 0.1$, $\alpha_R = 0.3$,

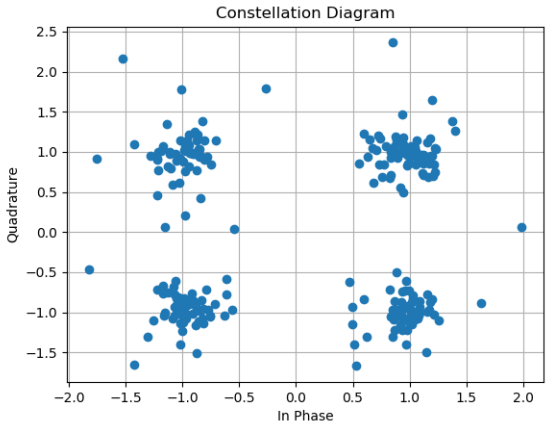


Fig. 6. Constellation using linear estimation

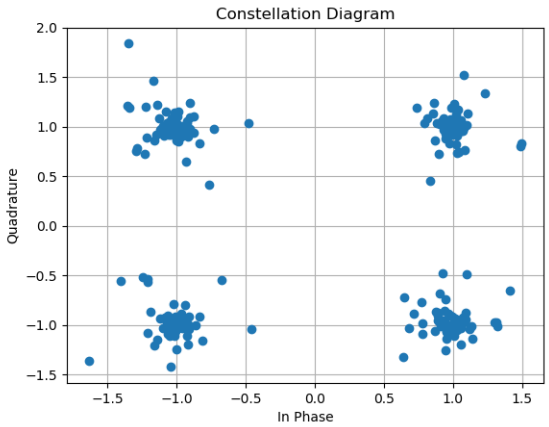


Fig. 7. Constellation using smart IQ estimation

$\phi_T = 0.2$, $\phi_R = 0.15$.

The symbol error rate is dependent on a few factors. First, the mixer imbalance parameters, $\alpha_T$, $\alpha_R$, $\phi_T$, $\phi_R$. The larger these values are, the more likely a symbol will be pushed over a decision boundary.

As constellation size increases, the symbols will be packed closer together, and the likelihood of a symbol error occurring increases.

## VII. Concluding Remarks

In this paper we improved on some earlier work for measuring and correcting mixer imbalance in OFDM direct to baseband systems. First we introduced two different, but equivalent, models for mixer imbalance commonly found in the literature. Then, using the symmetric model, we developed the equivalent frequency domain model and offered an intuitive visualization technique.

We improved on an existing unbiased estimator by taking advantage of symmetries that present themselves in our model. Our solution is also an unbiased estimator, but we are able to measure the channel matrix more precisely due to knowledge of these symmetries and therefore better equalize the channel effects. Results were shown in terms of constellation Error Vector Magnitude as SNR was varied for our estimator implementation as well as the implementation from earlier work and the traditional mixer unaware estimator.

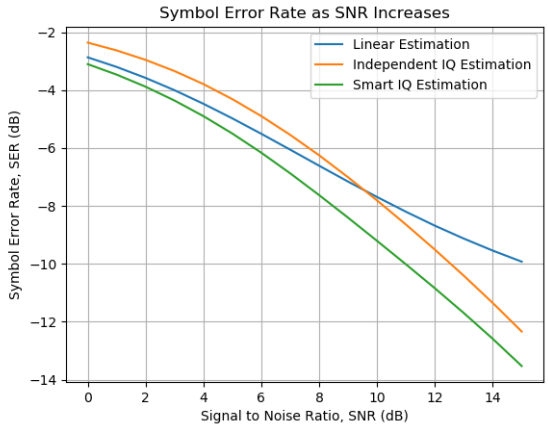


Fig. 8. Symbol error rate comparison of methods

Our methods can easily be expanded to work in MIMO architectures, in a way similar to that shown in other papers on competing methods [5, 8]. Although our models and simulations focused on frequency flat imbalance parameters, our methods will also work for wideband systems where the imbalance parameters may change accross the frequency band. Mixers of this sort are known to exist in the wild and come with datasheets showing measurements of imbalance over frequency [9].

## References

[1] N. A. Moseley, C. H. Slump, "A Low-complexity Feed-forward I/Q Imbalance Compensation Algorithm," *2006 Computational Statistics & Data Analysis - CS&DA*.

[2] I. Fatadin, S. J. Savory and D. Ives, "Compensation of Quadrature Imbalance in an Optical QPSK Coherent Receiver," in *IEEE Photonics Technology Letters*, vol. 20, no. 20, pp. 1733-1735, Oct.15, 2008, doi: 10.1109/LPT.2008.2004630.

[3] B. Razavi. *RF Microelectronics*. Englewood Cliffs, NJ: Prentice-Hall, 1998.

[4] A. A. Abidi, "Direct-conversion radio transceivers for digital communications," *IEEE J. Solid-State Circuits*, vol. 30, no. 12, pp. 1399–1410, Dec. 1995.

[5] Y. Zhu, C. Hall and A. Sayeed, "I-Q Mismatch Estimation and Compensation in Millimeter-Wave Wireless Systems," *2018 11th Global Symposium on Millimeter Waves (GSMM)*, Boulder, CO, USA, 2018, pp. 1-7, doi: 10.1109/GSMM.2018.8439206.

[6] S. M. Kay, *Fundamentals of statistical signal processing: estimation theory*. USA, Prentice-Hall, 1993.

[7] Stoer, Josef; Bulirsch, Roland (2002). *Introduction to Numerical Analysis* (3rd ed.)

[8] A. Tarighat, R. Bagheri and A. H. Sayed, "Compensation schemes and performance analysis of IQ imbalances in OFDM receivers," in *IEEE Transactions on Signal Processing*, vol. 53, no. 8, pp. 3257-3268, Aug. 2005, doi: 10.1109/TSP.2005.851156.

[9] Pasternack PE86X9005 Mixer Datasheet *https://www.pasternack.com/images/ProductPDF/PE86X9005.pdf*